J|A|C|S ARTICLES

Published on Web 01/21/2010

Nature of Bonding in Complexes Containing "Supershort" Metal−Metal Bonds. Raman and Theoretical Study of $M_2(dmp)_4$ [M = Cr (Natural Abundance Cr, ^{50}Cr, and ^{54}Cr) and Mo; dmp = 2,6-Dimethoxyphenyl]

Ryan E. Da Re,[#] Judith L. Eglin,[§] Christin N. Carlson,[§] Kevin D. John,*[,§] David E. Morris,[||] William H. Woodruff,[§] James A. Bailey,[▽] Enrique Batista,[⊥] Richard L. Martin,[⊥] F. Albert Cotton,[◆,†] Elizabeth A. Hillard,[¶] Carlos A. Murillo,[◆] Alfred P. Sattelberger,[○] and Robert J. Donohoe[§,‡]

Chemistry, Materials Physics and Applications, and Theory Divisions, Los Alamos National Laboratory, Los Alamos, New Mexico 87545, Advanced Engineering and Sciences, ITT Corporation, 2560 Huntington Avenue, Alexandria, Virginia 22303-1404, Chemistry, Earth & Environmental Sciences, Irving K. Barber School of Arts and Sciences, University of British Columbia Okanagan, 3333 University Way, Kelowna, BC Canada V1V 1V7, Argonne National Laboratory, 9700 South Cass Avenue, Argonne, Illinois 60439, Laboratory for Molecular Structure and Bonding, Department of Chemistry, P.O. Box 30012, Texas A&M University, College Station, Texas 77842-3012, and Laboratoire de Chimie et Biochimie des Complexes Moleculaires, Ecole Nationale Superieure de Chimie de Paris, UMR CNRS 7576, 11, rue Pierre et Marie Curie, 75231 Paris Cedex 05, France

Received July 16, 2009; E-mail: kjohn@lanl.gov

Abstract: We report an investigation of complexes of the type $M_2(dmp)_4$ (M = Mo, Cr; dmp = 2,6-dimethoxyphenyl) using resonance Raman (RR) spectroscopy, Cr isotopic substitution, and density functional theory (DFT) calculations. Assignment of the Mo−Mo stretching vibration in the Mo_2 species is straightforward, as evidenced by a single resonance-enhanced band at 424 cm^{-1}, consistent with an essentially unmixed metal−metal stretch, and overtones of this vibration. On the other hand, the Cr_2 congener has no obvious metal−metal stretching mode near 650−700 cm^{-1}, where empirical predictions based on the Cr−Cr distance as well as DFT calculations suggest that this vibration should appear if unmixed. Instead, three bands are observed at 345, 363, and 387 cm^{-1} that (a) have relative RR intensities that are sensitive to the Raman excitation frequency, (b) exhibit overtones and combinations in the RR spectra, and (c) shift in frequency upon isotopic substitution (^{50}Cr and ^{54}Cr). DFT calculations are used to model the vibrational data for the Mo_2 and Cr_2 systems. Both the DFT results and empirical predictions are in good agreement with experimental observations in the Mo_2 complex, but both, while mutually consistent, differ radically from experiment in the Cr_2 complex. Our experimental and theoretical results, especially the Cr isotope shifts, clearly demonstrate that the potential energy of the Cr−Cr stretching coordinate is distributed among several normal modes having both Cr−Cr and Cr−ligand character. The general significance of these results in interpreting spectroscopic observations in terms of the nature of metal−metal multiple bonding is discussed.

Introduction

Since the initial observations of multiple metal−metal bonding, there have been many spectroscopic and theoretical studies aimed at elucidating the nature of multiple bonding in general and the quadruple bond between d^4 transition metals in particular. Specifically, while quadruple bonding is relatively well characterized for complexes of the later Group VIB elements, $Mo(II)_2$ and $W(II)_2$,[1] there is more uncertainty about the nature of the bonding in the $Cr(II)_2$ analogues, including those with "supershort" Cr−Cr bonds.[2] It is a fundamental challenge to our understanding of chemical bonding to determine what factors govern these chromium−chromium interactions and

[§] Chemistry Division, LANL.
[||] Materials Physics and Applications Division, LANL.
[⊥] Theory Division, LANL.
[#] ITT Corp.
[▽] UBC Okanagan.
[○] Argonne National Laboratory.
[◆] Texas A&M University.
[¶] Ecole Nationale Superieure de Chimie de Paris.
[†] Deceased February 20, 2007.
[‡] Deceased April 26, 2007.

(1) Cotton, F. A.; Murillo, C. A.; Walton, R. A. *Multiple Bonds Between Metal Atoms*, 3rd ed.; Springer Science: New York, 2005.
(2) (a) Cotton, F. A.; Hanson, B. E.; Rice, G. W. *Angew. Chem., Int. Ed. Engl.* **1978**, *17*, 953. (b) Bino, A.; Cotton, F. A.; Kaim, W. *Inorg. Chem.* **1979**, *18*, 3030. (c) Bino, A.; Cotton, F. A.; Kaim, W. *Inorg. Chem.* **1979**, *18*, 3566. (d) Bino, A.; Cotton, F. A.; Kaim, W. *J. Am. Chem. Soc.* **1979**, *101*, 2506. (e) Cotton, F. A.; Hillard, H. A.; Murillo, C. A.; Zhou, H. C. *J. Am. Chem. Soc.* **2000**, *122*, 416.

how they should be modeled.[3] Realistic experimental determination of the bonding in such complexes is equally challenging.

Single-crystal optical analysis on $Cr_2(O_2CCH_3)_4 \cdot 2H_2O$ (which has a Cr−Cr bond distance of 1.966 Å) suggested that the lowest energy electronic transition of this complex was due to a $\delta \rightarrow \pi^*$ transition, not $\delta \rightarrow \delta^*$ as is the case for most quadruply bonded complexes.[4] The ground-state Cr−Cr stretch was estimated on the basis of excited-state vibronic analysis of this transition and other low-energy states to be in the 150−250 cm^{-1} range (force constant range 0.35−0.96 mdyn/Å; the diatomic approximation, *vide infra*, is used to estimate force constants from frequencies in all cases herein unless otherwise stated). These force constant values are extremely low for a metal−metal quadruple bond. For example, the M−M stretch values reported for the non-axially ligated congeners $Mo_2(O_2CCH_3)_4$[5] and $W_2(O_2CCH_3)_4$[6] are 404 cm^{-1} (Mo−Mo bond distance 2.09 Å, force constant 4.62 mdyn/Å) and 304 cm^{-1} (W−W bond distance 2.22 Å, 5.02 mdyn/Å), respectively.[7] Of the "supershort" class of quadruply bonded Cr(II) complexes, only one ligand set has been characterized by electronic/vibrational spectroscopy prior to this report. Cotton et al. originally reported that $\nu(Cr_2)$ for $Cr_2(mhp)_4$ (mhp = deprotonated 6-methyl-2-hydroxypyridine)[8a] was 556 cm^{-1} (Cr−Cr bond distance 1.889 Å, 4.74 mdyn/Å).

Numerous empirical relationships between force constants and bond distances have been proposed by many workers over the past eight decades.[9−16] These "CNPE" (Complete Neglect of Practically Everything[14]) relationships differ in mathematical form and in range of applicability depending on the experimental data available at the time the relationship was devised and the type of systems addressed by the investigators. However, all of them embody the same general observation: that force constants increase monotonically with decreasing bond distance. This fact is independent of state of matter, electronic state, molecular complexity, formal bond order, etc. (as shown in Figure 1 for the rows of the Periodic Table containing the first and second transition series) and requires only that the correlation be drawn for bonds between elements in the same row of the Periodic Table.[17] There are several great advantages to these empirical rules, paramount among which is the direct relationship that they establish between spectroscopic observables (vibrational frequencies) and structure. Second, the rules offer a simple sanity test for vibrational assignments: while the correlations have experimental scatter, any putative assignment that differs substantially from the empirical prediction should be viewed with caution and examined critically.

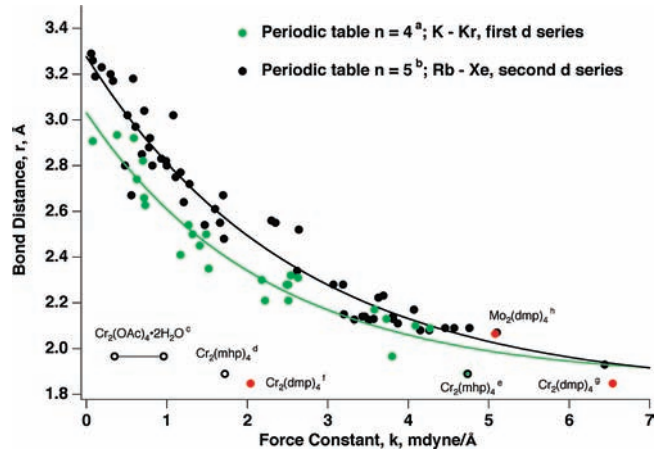

Figure 1. Empirical correlations between force constants and bond distances for elements in the rows of the Periodic Table containing the first transition series (principle quantum number 4, green points) and the second transition series (principal quantum number 5, black points). Solid lines are exponential decay fits to the empirical data other than that from the present work, see ref 16. Open circles represent work by others on Cr complexes where assignment of the Cr−Cr stretching frequency is an issue. Red points are from the present work. [a]Identity of $n = 4$ points in order of decreasing bond distance: Ti (metal), $Mn_2(CO)_{10}$, Zn (metal), KBr (s), $Co_2(MeNC)_{10}$, Br_2 (gas, $^3\Pi u$,^1u), Br_2 (gas, $^3\Pi u$,Ou^+), Zn′ (metal), V (metal), Br_3^- (aq), As_2 (gas, $^1\Sigma u^+$), As_2 (gas, $^1\Sigma u^-$), Se_2 (gas, $^3\Sigma g$), Ge_2H_6, GaBr (s), $TiBr_4$ (l), $GeBr_4$ (s), As_2 (gas, $^3\Sigma u^+$), As_2 (gas, $^3\Sigma u^-$), Br_2 (l), As_2 ($^3\Pi g$), $ZnBr_2$ (s), Se_2 (gas, Og^+), GeSe (gas, $^1\Sigma^+$), As_2 (gas, $^1\Sigma g^+$), Se_2 (gas, $^3\Sigma u^-$), $Cr_2(OAc)_4$ (s), $Cr_2(mhp)_4$. [b]Identity of $n = 5$ points given in ref 15. [c]$Cr_2(OAc)_4 \cdot 2H_2O$ from ref 4, frequency range shown. [d]$Cr_2(mhp)_4$, frequency from ref 15. [e]$Cr_2(mhp)_4$, frequency from ref 8a. [f]$Cr_2(dmp)_4$, present work, frequency assumed to be the average of bands a, b, and c (365 cm^{-1}), see text. [g]$Cr_2(dmp)_4$, present work, frequency estimated from isotope shifts (650 cm^{-1}), see text. [h]$Mo_2(dmp)_4$, frequency as measured (424 cm^{-1}), present work.

The value reported by Cotton et al. for the Cr−Cr stretching frequency in $Cr_2(mhp)_4$, 556 cm^{-1},[8a] is in accord with expectation based upon the application of a simple diatomic oscillator approximation for an unmixed Cr−Cr coordinate where the force constant is ∼5 mdyn/Å. This force constant is, in turn, in approximate agreement with the prediction from the Cr−Cr bond distance (1.889 Å) in $Cr_2(mhp)_4$, using the empirical relationships developed by Woodruff et al. (see Figure 1).[16] On the other hand, Manning and Trogler determined that $\nu(Cr_2)$ for this complex is most likely to be either 340 or 400 cm^{-1} on the basis of vibronic features in the absorption and emission spectra and combined infrared and Raman analysis of the same complex.[18] In particular, observation of a ∼320 cm^{-1} vibronic progression in the nominal $\delta \rightarrow \delta^*$ excited state led Manning and Trogler to suggest that 340 cm^{-1} (1.72 mdyn/Å) was likely to be the ground-state Cr_2 stretch, as a 10−15% reduction in $\nu(M_2)$ is typically observed in the excited state for quadruply

(3) (a) Goodgame, M. M.; Goddard, W. A. *Phys. Rev. Lett.* **1982**, *48*, 135. (b) Edgecombe, K. E.; Becke, A. D. *Chem. Phys. Lett.* **1995**, *244*, 427. (c) Horvath, S.; Gorelsky, S. I.; Gambarotta, S.; Korobkov, I. *Angew. Chem., Int. Ed.* **2008**, *47*, 9937.
(4) Rice, S. F.; Wilson, R. B.; Solomon, E. I. *Inorg. Chem.* **1980**, *19*, 3425.
(5) (a) Bratton, W. K.; Cotton, F. A.; Debeau, M.; Walton, R. A. *J. Coord. Chem.* **1971**, *1*, 121. (b) San Fillipo, J., Jr.; Sniadoch, H. J. *Inorg. Chem.* **1973**, *12*, 2326. (c) Ketteringham, A. P.; Oldham, C. *J. Chem. Soc., Dalton Trans.* **1973**, 1067. (d) Clark, R. J. H.; Hempleman, A. J.; Kurmoo, M. *J. Chem. Soc., Dalton Trans.* **1988**, 973.
(6) Santure, D. J.; Huffman, J. C.; Sattelberger, A. P. *Inorg. Chem.* **1985**, *24*, 371.
(7) Note, however, that in the case of $Cr_2(O_2CCH_3)_4 \cdot 2H_2O$ there will be obligatory kinematic coupling between the Cr−Cr coordinate and the symmetric Cr−OH_2 coordinate involving the axial waters, so a pure Cr−Cr normal vibrational mode is not expected.
(8) (a) Cotton, F. A.; Fanwick, P. R.; Niswander, R. H.; Sekutowski, J. C. *J. Am. Chem. Soc.* **1978**, *100*, 4725. (b) Cotton, F. A.; Koch, S. A.; Millar, M. *Inorg. Chem.* **1978**, *17*, 2087.
(9) Badger, R. M. *J. Chem. Phys.* **1934**, *2*, 128.
(10) Badger, R. M. *Phys. Rev.* **1935**, *48*, 284.
(11) Badger, R. M. *J. Chem. Phys.* **1935**, *3*, 710.
(12) Pauling, L. *Phys. Rev.* **1938**, *54*, 899.
(13) Herschbach, D. R.; Laurie, V. *W J. Chem. Phys.* **1961**, *35*, 458.
(14) Buergi, H. B.; Dunitz, J. D. *J. Am. Chem. Soc.* **1987**, *109*, 2924.
(15) Miskowski, V. M.; Dallinger, R. F.; Christoph, G. G.; Morris, D. E.; Spies, G. H.; Woodruff, W. H. *Inorg. Chem.* **1987**, *26*, 2127.
(16) Dyer, R. B.; Woodruff, W. H. Vibrational Spectroscopy. In *Encyclopedia of Inorganic Chemistry Methods and Applications*, Vol. 1, Applications of Physical Methods to Inorganic and Bioinorganic Chemistry; Scott, R. A., Ed.; Wiley: New York, 2007; pp 489−512.
(17) While these rules are quite general, exceptions are expected for certain distorted interatomic potentials, such as double minima.
(18) Manning, M. C.; Trogler, W. C. *J. Am. Chem. Soc.* **1983**, *105*, 5311.

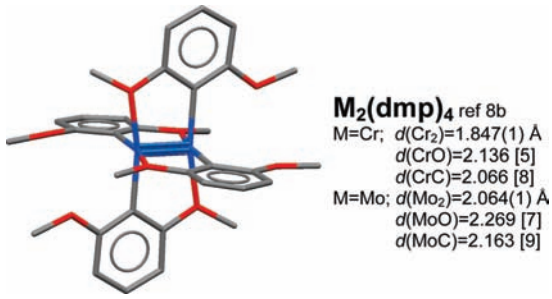

Figure 2. Ligand arrangements and geometric parameters in $M_2(dmp)_4$.

bonded M_2 systems. This result would suggest that the Cr_2 quadruple bond is much weaker in $Cr_2(mhp)_4$ (1.72 mdyn/Å) than expected on the basis of the empirical relationships with bond distance (4.74 mdyn/Å). A similar apparent conflict between experimental observations and empirical predictions was noted above for $Cr_2(O_2CCH_3)_4 \cdot 2H_2O$.

In this paper we report electronic and Raman spectra of $M_2(dmp)_4$ (M = Cr, Mo; dmp = 2,6-dimethoxyphenyl), including excitation-energy-dependent resonance Raman (RR) intensity profiles, chromium isotopic substitutions, and electronic absorption spectra (Figure 2). We also report hybrid density functional theory (DFT) calculations, which provide accurate estimates of the M−L and M−M stretching frequencies for the $Mo_2(dmp)_4$ complex but appear to conflict with experimental observations on $Cr_2(dmp)_4$.

Experimental Details

Syntheses. All reactions and product manipulations were carried out under an atmosphere of dry nitrogen using standard drybox or Schlenk techniques. Anhydrous solvents, tetrahydrofuran (THF), toluene, and methylene chloride were purchased from Aldrich or Acros and stored in a glovebox over activated 4 Å molecular sieves overnight, and passed the ketyl test before use. Chromium isotopes (^{50}Cr and ^{54}Cr) in the form of metal/metal oxide were obtained from Oak Ridge National Laboratory's Stable Isotope Program and used as received. $Mo_2(dmp)_4$ was prepared according to the literature procedure.[8b]

$Cr_2(O_2CCH_3)_4$. Chromium metal (100 mg, 2 mmol) was digested in 6 mL of 6 M aqueous HCl with the evolution of H_2(g).[19] After several days and complete dissolution of the metal, the green Cr(III) solution was then poured into a Schlenk flask containing amalgamated Zn. The Zn amalgam was prepared by adding 3 mL of 1 M aqueous HCl to 50−100 mg of mercury chloride and 1 g of 30 mesh zinc metal for 5 min and then rinsing with water.[20] After stirring under nitrogen for 1 h, the green Cr(III) solution turned blue with the formation of Cr(II).

In a Schlenk tube, 4 g (49 mmol) of sodium acetate was dissolved in 10 mL of degassed water. The Cr(II) solution was layered over the sodium acetate solution, and slow diffusion resulted in large, red crystals of $Cr_2(O_2CCH_3)_4 \cdot 2H_2O$. The solution was chilled to 0 °C before the supernatant was removed. The $Cr_2(O_2CCH_3)_4 \cdot 2H_2O$ was heated in a water bath under vacuum, resulting in brown $Cr_2(O_2CCH_3)_4$ (0.21 g, 95.7% yield). Reactions performed with $^{50}Cr^0$ and $^{54}Cr^0$ resulted in 0.018 g (8.2%) and 0.078 g (35.6%) of $^{50}Cr_2(O_2CCH_3)_4$ and $^{54}Cr_2(O_2CCH_3)_4$, respectively. Low yields indicated the presence of other components in the isotopically enriched stock material, as confirmed by semiquantitative mass spectrometry and powder X-ray diffraction studies.

$Cr_2(dmp)_4$. $^{50}Cr_2(dmp)_4$ and $^{54}Cr_2(dmp)_4$ were synthesized in a drybox under nitrogen as previously reported using $^{50}Cr_2(O_2CCH_3)_4$ and $^{54}Cr_2(O_2CCH_3)_4$, respectively, as the starting materials.[8b]

Electronic Absorption Spectroscopy. Absorption spectra for the Cr and Mo complexes were collected from 2-methyl-THF solutions at room temperature and 15 K, and for the Cr complex at 77 K.

Raman Spectroscopy. Raman spectra were collected from powder samples in sealed capillary tubes at room temperature. Similar spectra were observed for samples at 77 K or at room temperature in THF, with minor alterations as detailed below. Laser excitation for the data shown herein was provided by a commercial argon ion or HeNe laser, or a CW Nd:YVO_4 source, the last of which was integrated into a commercial Fourier transform (FT) Raman instrument. For the first two sources, the incident light was focused onto the samples in a 135° backscattering geometry at power levels between 1 and 20 mW. The Mo sample exhibited extensive photodecomposition with 488 nm excitation, and power levels with the other visible lines were maintained <10 mW. The scattered light was coupled into either a commercial triple-stage or single-stage spectrograph. In the latter case a holographic notch filter was used to reduce the Rayleigh intensity. The Raman shifs were calibrated by the use of 50:50 toluene/acetonitrile or 4-acetamidophenol using the data compiled by the McCreery group (http://www.chemistry.ohio-state.edu/~rmccreer/freqcorr/shift.html). Acquisition of the entire spectral region (200−1600 cm^{-1}) required superposition of varying numbers of spectrographic windows, from two for 458 nm excitation to seven for 633 nm. In order to maintain accurate relative intensities of the Raman peaks, each spectral window included a relatively intense peak from adjoining windows. The final spectra as shown include concatenation of multiple windows and baseline correction using a spline fitting procedure.

Computational Details. DFT calculations employed the B3LYP hybrid approximation as implemented in the Gaussian09 suite of programs.[21] The Cr atom was described with an all-electron basis which is of triple-ζ character in the valence space and includes an additional set of diffuse s, p, and d functions and a single f-type polarization function (6-311+G*). The Mo centers were described by the Hay−Wadt relativistic effective core potential and the associated LANL08 basis set.[22] All other atoms utilized the 6-31G* basis.

Results and Discussion

Theoretical Description. A quantitative description of metal−metal multiple bonds has long been a challenge for theory. The basic problem is that we must treat two extremes in bonding − the strong interaction molecular orbital limit characteristic of the σ-bond and the weak interaction valence bond limit appropriate for the δ-bond − equitably within a single approximation. This is a tall order for any single-determinant-based approximation, such as DFT. Multideterminant descriptions, such as the complete-active-space (CAS) approximation, are better equipped to describe the character of the wave function, but these approaches have their own problems, especially the well-known overestimation of the intraorbital Coulomb repulsion (the Hubbard U parameter) which accompanies a configuration expansion based on Hartree−Fock orbitals. In this section we describe efforts to provide some support for the interpretation of the spectroscopy using hybrid density functional theory.

(19) Holah, D. G.; Fackler, J. P. In *Inorganic Synthesis*, Vol. X; Muetterties, E. L., Ed.; McGraw-Hill Book Co.: New York, 1967; p26.
(20) Ocone, L. R.; Block, B. P. In *Inorganic Synthesis*, Vol. VIII; Audrieth, L. F., Bailar, J. C., Fernelius, W. C., Johnson, W. C., Kleinberg, J., Moeller, T., Rochow, E. G., Schumband, W. C., Young, R. C., Eds.; McGraw-Hill Book Co.: New York, 1966; p125.
(21) Frisch, M. J.; et al. *Gaussian 09*, Revision A.02; Gaussian, Inc.: Wallingford CT, 2009.
(22) (a) Hay, P. J.; Wadt, W. R. *J. Chem. Phys.* **1985**, *82*, 299. (b) Roy, L. E.; Hay, P. J.; Martin, R. L. *J. Comput. Theor. Chem.* **2008**, *4*, 1029.

Table 1. Geometric Parameters Characterizing the B3LYP Optimum Geometries for the Quadruple Bonded States[a]

S	*ρ*	*d*(M−M)	*d*(M−O)	*d*(M−C)	*ν*(M−M)
			$Cr_2(dmp)_4$		
0	NA	1.70	2.17	2.06	483 (2%)
					644 (53%)
					670 (42%)
1	0.99	1.79	2.18	2.07	476 (5%)
					587 (83%)
					597 (8%)
			$Mo_2(dmp)_4$		
0	NA	2.10	2.35	2.15	449 (50%, 136)
					456 (12%, 12)
					504 (38%, 23)
1	0.52	2.16	2.38	2.16	431 (75%)
					494 (23%)

[a] Distances are reported in Å. Significant metal−metal stretching motion is found in two modes, see text. The square of the overlap of the diatomic metal−metal stretch with the normal mode and the Raman activity (Å^4/amu) are given parenthetically.

We begin the discussion with the Mo dimer, $Mo_2(dmp)_4$. Geometric parameters characterizing the B3LYP closed-shell singlet, corresponding to the formal quadruple bond, are given in Table 1. Note that the Mo−Mo bond length is in reasonable agreement with the experimental distance (2.10 Å calculated vs 2.064(1) Å measured). We also investigated the possibility that there might be a "weakly coupled", valence-bond-like state. We found no evidence for this in the B3LYP approximation; direct computation of the orbital mixing Hessian showed the closed-shell singlet to be stable to both orbital and spin instabilities. An explicit self-consistent field (SCF) calculation on the lowest triplet state generated by uncoupling the two electrons occupying the δ-orbital places it some 10.0 kcal/mol above the closed-shell ground state. Half this value, or 5 kcal/mol, is a crude measure of the strength of the δ-bond in this species according to the B3LYP functional.[23] The Mo−Mo bond distance increases some 0.06 Å in the triplet state, providing a rough measure of the bond length contraction associated with the δ-bond. The vibrational normal modes of the ground-state singlet show significant projections onto the basic Mo−Mo internal stretching coordinate in two of the computed normal modes, one at 449 cm^{-1} and the other at 504 cm^{-1}. The parentage of the simple Mo−Mo internal coordinate in these two modes is 50% and 38%, respectively. This is in good agreement with experiment, where the dominant RR feature associated with disruption of the δ-bond is seen at 424 cm^{-1}. These modes can be found at 431 (75%) and 494 cm^{-1} (23%) in the triplet $\delta\rightarrow\delta^*$ excited state, a reduction in the dominant mode of some 4% relative to the singlet ground state. As the spectral features associated with the Mo−Mo complex seem to be in good agreement with the properties of the closed-shell ground state, no further attention was devoted to this system.

The description of $Cr_2(dmp)_4$ using DFT is expected to be only semiquantitative at best on the basis of the similarity of this quadruply bonded system to the formal sextuple bond in Cr_2. First transition series metal−metal interactions, especially the weakly overlapping $\delta-\delta$ interactions, are influenced much more by the small d-orbital radius and consequent large electron−electron repulsion than are the interactions of the "softer" second- and third-row metals. This on-site repulsion is unavoidable in a single determinant description of the ground state, and so the more flexible CAS method, or its perturbation theory improvement, CAS-PT2, is preferred. Unfortunately, the packages available to us either did not implement or were not capable of the analytic second derivative calculations needed to study frequencies. These are available within DFT approximations, and so we hoped they might provide some guidance for our assignments.

(23) This is the vertical excitation energy. The unpaired Mulliken spin density is dominantly in the metal d-orbitals ($\rho_{Mo} = 0.88$). If the geometry of the triplet state is allowed to relax, the energy difference is reduced slightly to 9.9 kcal/mol. The Mo−Mo, Mo−O, and Mo−C distances in the triplet are 2.16, 2.37, and 2.16 Å, respectively.

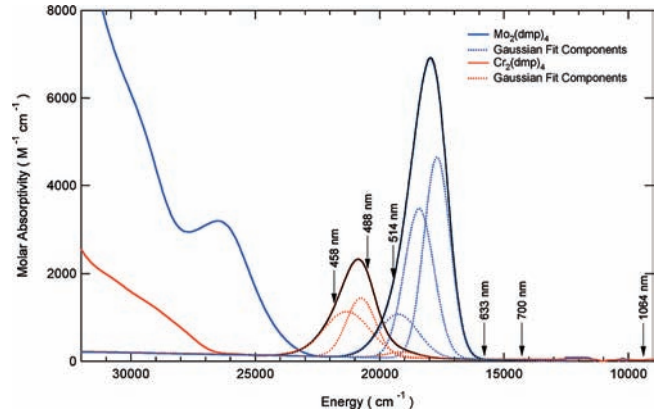

Figure 3. Electronic absorption spectra of $Mo_2(dmp)_4$ and $Cr_2(dmp)_4$ in THF solution at room temperature. Gaussian fits are also shown (dashed lines).

The first indication of problems with the B3LYP description of $Cr_2(dmp)_4$ can be seen in the computed Cr−Cr distance. The bond distance for the closed-shell singlet is significantly shorter than experiment, 1.70 vs 1.849(2) Å. This implies that B3LYP is overemphasizing the extent of the bonding. In fact, time-dependent (TD) DFT calculations on the Cr dimer do exhibit a triplet instability. That is, at the optimum geometry of the closed-shell singlet, the TDDFT approximation predicts a lower-lying triplet state, corresponding to breaking the δ-bond in favor of a $\delta\rightarrow\delta^*$ triplet state. This prediction was verified by an explicit SCF calculation on the $\delta\rightarrow\delta^*$ triplet state, which places the triplet slightly below (−1.1 kcal/mol) the closed-shell (δ^2) singlet. The energies of higher spin states (quintet, septet, etc.) were also examined, but all were found to be higher in energy than either the singlet or triplet. If the triplet state is allowed to relax its geometry, the Cr−Cr bond lengthens significantly to 1.79 from 1.70 Å at the closed-shell geometry. Measured from their respective minima, the triplet lies 5 kcal/mol lower than the singlet. Here we note that the weak, low-energy feature in the Gaussian resolution of the $Cr_2(dmp)_4$ electronic absorption spectrum (Figure 3) lies approximately 0.2 eV or 4.6 kcal below the next-higher-energy Gaussian component of the absorption envelope. The Cr−Cr stretch in the δ^2 singlet is found predominantly in the region 644−670 cm^{-1}. This shifts downward by ∼10% to 587 cm^{-1} in the triplet $\delta\rightarrow\delta^*$ state, in agreement with the expectation of Manning and Trogler.[18]

We examined one final limiting case for the Cr dimer. The B3LYP preference for the triplet state suggests that this system may be closer to the valence bond limit than the molecular orbital (quadruple bond) limit. To address this question, we examined a broken-symmetry, "anti-ferromagnetic", valence-bond singlet. It corresponds conceptually to coupling four electrons on each metal site high spin ($S = 2$), and subsequently coupling those $S = 2$ moments anti-ferromagnetically. At the optimum geometry of the triplet $\delta\rightarrow\delta^*$ state, this broken-symmetry state is 17.8 kcal/mol lower in energy than the triplet.

The unpaired spin density on each Cr site ($\rho = 3.86$) basically corresponds to two high-spin d^4 Cr atoms, coupled. Attempts to optimize the geometry of this determinant proved difficult. Subsequent geometrical steps, even when using the full analytic Hessian, reverted to the closed-shell solution, which then optimizes to the geometry discussed previously.

Electronic Spectra. The absorption spectra in THF solution at room temperature for the $Cr_2(dmp)_4$ and $Mo_2(dmp)_4$ complexes are shown in Figure 3. Considering only the lowest-energy absorption features, which are expected to contain the $\delta\rightarrow\delta^*$ transition, the room-temperature spectra show peaks at 17 796 cm^{-1} (556 nm) for $Mo_2(dmp)_4$ and 20 833 cm^{-1} (480 nm) for $Cr_2(dmp)_4$. In neither the Cr nor Mo complexes can this absorption envelope be fit by a simple, single Gaussian; the Gaussian components underlying the two absorption envelopes are also shown in Figure 3. In the Mo complex these components appear at 17 690 (565 nm), 18 410 (543 nm), and 19 250 cm^{-1} (519 nm). In the Cr complex the Gaussian components appear at 19 070 (524 nm), 20 750 (482 nm), and 21 315 cm^{-1} (469 nm). The 19 070 cm^{-1} Gaussian component of the Cr spectrum is notable for several reasons: it has no obvious analogue in the Mo spectrum, it is much weaker than any of the other components of either spectrum, and it is separated from the nearest component of the Cr spectrum by the greatest frequency difference (1680 cm^{-1}) of any of the other component spacings in either the Cr or Mo spectra. The remaining two components of the Cr spectrum are separated by 565 cm^{-1}, and the Mo spacings are 720 and 840 cm^{-1}. Absorption spectra taken at 15 K (see Supporting Information) exhibit vibronic progressions for both the Cr and Mo complexes. The progression spacing averages 330 cm^{-1} in the Mo complex and 290 cm^{-1} in the Cr complex. Accordingly, the multiple Gaussian components observed at room temperature cannot be single-quantum vibronic progressions involving the same mode(s) observed in the 15 K spectra. The similarity of the vibronic progressions observed in the 15 K electronic spectrum of $Cr_2(dmp)_4$ and in the $Mo_2(dmp)_4$ complex, where the resonant electronic transition is unambiguously $\delta\rightarrow\delta^*$, suggests that the lowest-energy intense contributor to the electronic absorption envelope of both the Cr and Mo complexes is $\delta\rightarrow\delta^*$.

In the $\delta\rightarrow\delta^*$ excited state of the Cr−Cr moiety, both the spatial extent and the energetics of the δ-orbitals are altered. Thus, so is the metal−ligand $d\pi-p\pi$ bonding as well as the π-electron density on the phenyl ring and in turn the Cr−C coordinate and internal interatomic coordinates of the phenyl ring. Through this type of mechanism, given strong metal−ligand $d\pi-p\pi$ bonding in the first place, $\delta\rightarrow\delta^*$ excitation will result in Franck−Condon resonance enhancement of both Cr−C and internal phenyl ring modes without the necessity to invoke a distinct metal-to-ligand or ligand-to-metal charge-transfer (MLCT or LMCT) transition. We suggest that this is indeed the case in $Cr_2(dmp)_4$, and that similar metal−ligand $d\pi-p\pi$ bonding may be responsible for previous observations of apparently anomalous spectroscopic behavior in chromium complexes having formal quadruple bonds.[4,17]

Raman Spectra. Figure 3 also shows the six different laser excitation frequencies used to obtain Raman (and RR) spectra in the course of this study. These range from near-infrared (1064 nm, 9399 cm^{-1}), far from any resonant electronic transitions of the complexes, through the absorption envelopes discussed above. All of the peaks in the Raman spectra are polarized ($0.1 < \rho < 0.5$) and thus are due to symmetric (A_g) vibrations of these complexes, which have C_{2h} symmetry. The 1064-nm-excited Raman spectra of the free dmp ligand plus the Cr and Mo complexes are shown in Figure 4. All three spectra are similar above 700 cm^{-1}, with some notable effects of metal coordination. Several ligand modes, most obviously the phenyl ring modes at 989, 1170, and 1223 cm^{-1} in the free ligand, are upshifted in the complexes. Additionally, several ligand modes are split into two components in the Cr complex but not Mo. This shows that Cr exerts a perturbation on the ligand set that is absent in the Mo complex, which suggests that metal−ligand electronic interactions involving the phenyl π-orbitals and the metal δ-orbitals (having π symmetry with respect to the ligands) are stronger for Cr than for Mo.

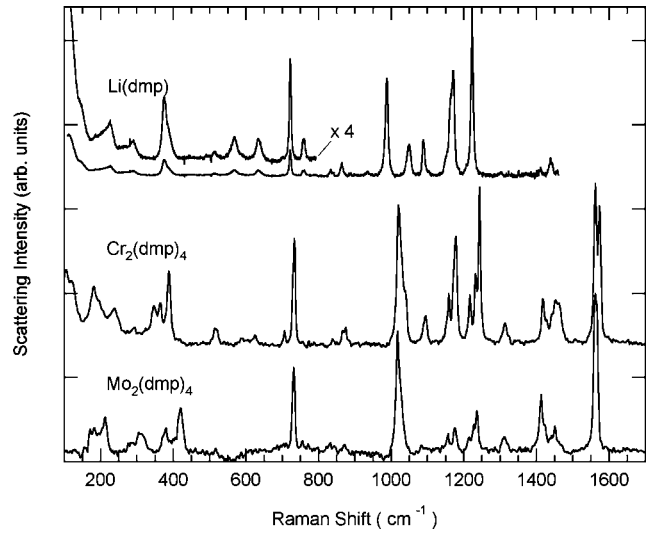

Figure 4. FT Raman (1064 nm) spectra of LiDMP, $Cr_2(dmp)_4$, and $Mo_2(dmp)_4$.

The spectral region below 500 cm^{-1} in Figure 4 reinforces the idea that Cr perturbs the electronic and vibrational structure of the dmp ligands much more strongly than does Mo. The low-frequency modes observed for the free ligand spectrum can all be correlated with peaks in the spectrum of the Mo complex; in addition, the Mo complex shows several new peaks that can be ascribed to metal−ligand or metal−metal modes. In the Cr spectrum, however, the low-frequency ligand spectrum is virtually unrecognizable. Obviously, coordination to Cr affects the dmp ligand in ways that coordination to Mo does not, again bespeaking uniquely strong Cr−dmp electronic interactions.

The dependences of the Raman spectra from $Mo_2(dmp)_4$ and $Cr_2(dmp)_4$ upon laser excitation wavelength are shown in Figures 5 and 6, respectively. When excited far from resonance (1064 nm), as noted above, both species exhibit a complex Raman spectrum, dominated by dmp ligand modes. These bands are generally 2−8 cm^{-1} higher frequency than in the free ligand and, for modes assigned to the aromatic ring, split in the Cr complex.

With visible excitation, the molybdenum sample yields a relatively simple spectrum dominated by a fundamental band (424 cm^{-1}) and, with 514 nm excitation, at least two overtone bands, which are readily assigned to the metal−metal stretching mode (force constant 5.08 mdyn/Å). This is entirely consistent with the empirical prediction for this row of the Periodic Table (Figure 1, 405 cm^{-1}) for high-order metal−metal bonds[15] and also the DFT calculations (449 cm^{-1}). Thus the Raman data, like the vibronic spectra, strongly support the assignment of one of the Gaussian components of the visible absorption for the $Mo_2(dmp)_4$ complex to a $\delta\rightarrow\delta^*$ transition.

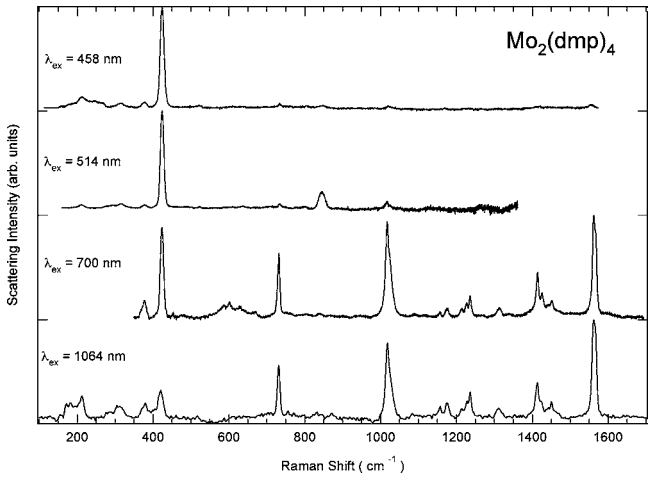

Figure 5. FT Raman (1064 nm) and resonance Raman (458, 514, and 700 nm) spectra of $Mo_2(dmp)_4$.

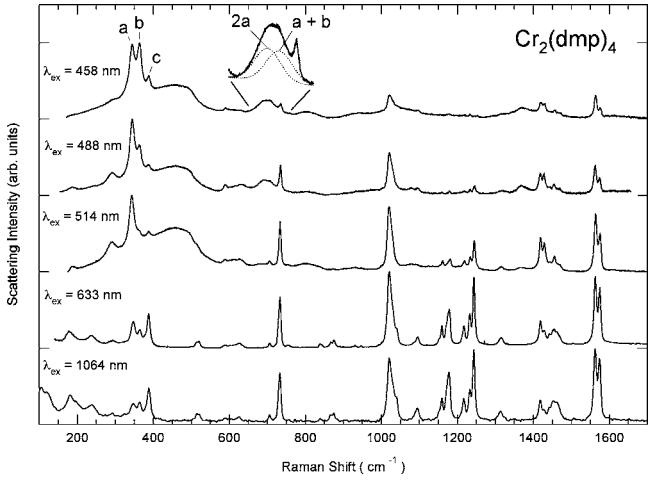

Figure 6. FT Raman (1064 nm) and resonance Raman (458, 488, 514, and 633 nm) spectra of $Cr_2(dmp)_4$.

It is virtually certain that the dominant, lowest-energy component, which also shows the vibronic progression at 15 K of ca. 330 cm^{-1}, a perfectly reasonable value for the excited-state Mo−Mo stretch, is in fact the $\delta\rightarrow\delta^*$ transition. The relative simplicity of the visible−excitation data, i.e., the prominent RR peak at 424 cm^{-1} and its overtones and combinations, demonstrates that the primary source of vibronic coupling in the optical absorption arises from the metal−metal stretching coordinate via a Franck−Condon resonance enhancement mechanism,[24] where the primary coordinate displaced upon electronic excitation is the Mo−Mo distance. While there is no evidence in either the RR or vibronic spectra of strong coupling, either kinematic or electronic, of internal dmp ligand modes to the metal−metal stretching mode, we do observe low-frequency vibrations at 212, 293, 314, and 378 cm^{-1} that we assign as metal−ligand stretches and angle bends, as evidenced by weak $\delta\rightarrow\delta^*$ resonance enhancement and the observation of weak overtones and combinations at 587, 602, 607, and 628 cm^{-1}. The two higher-energy Gaussian components of the electronic absorption envelope are most likely vibronic sidebands on the $\delta\rightarrow\delta^*$ transition. The alternative assignment, δ(Mo)−π^*(dmp) MLCT or LMCT, seems to be eliminated because no $\delta\rightarrow\delta^*$ resonance enhancement of dmp phenyl ring modes is observed.

The excitation dependence from $Cr_2(dmp)_4$ is much more complicated, including three general patterns of relative intensity change with excitation wavelength. The first intensity pattern is seen in the behavior of the five bands straddling the 1200 cm^{-1} Raman shift, two immediately below and three immediately above. These bands lose intensity relative to all other spectral features as the excitation is tuned toward the blue and resonant with the visible absorption. The frequencies of this group are typical of carbon−oxygen single bonds. Thus, we attribute these bands to methoxy group vibrations of the ligand and consider their intensities to provide something of an internal standard for non-resonance-enhanced behavior. A second pattern is associated with the phenyl ring modes at 1564, 1021, and 734 cm^{-1}, as well as other ring modes. These bands gain intensity compared with the first group but lose intensity compared with the third group, which comprises three bands at 345, 363, and 387 cm^{-1} and overtones and combinations involving these fundamentals. These are assigned as normal modes composed of contributions from metal−metal stretching, metal−ligand stretching, or metal−metal−ligand bending internal coordinates. We designate the three fundamentals as bands a, b, and c. This set of bands exhibits an increase in relative intensity compared with all other bands as the excitation is tuned toward the blue. Other members of this last group include a broad peak near 700 cm^{-1}, which can be resolved (Figure 6) into an overtone of the band at 690 cm^{-1} and the combination of bands a + b at 708 cm^{-1}.

Additionally, in RR spectra taken at 77 K using 514.5 nm excitation (data not shown), the fundamental bands a, b, and c upshift by approximately 5 cm^{-1} and the overtone/combination envelope shifts up by approximately 10 cm^{-1}. Peak resolution of the 77 K overtone/combination envelope reveals two contributing Lorenzian peaks centered at 698 and 712 cm^{-1}, confirming the room-temperature assignments to the overtone (2×349 cm^{-1}) and the combination ($349 + 367$ cm^{-1}). Peaks are also observed at 1079 and 1368 cm^{-1}, which are assigned as combinations of the aromatic ring distortion and trigonal breathing modes at 734 and 1021 cm^{-1}, respectively,[25] with band a. These observations might suggest a Cr−Cr stretching frequency in $Cr_2(dmp)_4$ near 365 cm^{-1}, but this frequency is quite inconsistent with the empirical data in Figure 1 and with the DFT calculations.

Interestingly, the intensities of bands a, b, and c *relative to one another* change dramatically throughout the series of excitation wavelengths (Figure 6). Finally (not shown), band b in this group shifts by 4 cm^{-1} to lower energy in THF solution compared to powder RR spectra, while the others remain unchanged. The spectra in THF also show a low-frequency peak (187 cm^{-1} in the normal isotopic sample) that is missing in the powder spectra and thus can be definitively ascribed to a normal mode composed primarily of the symmetric O−Cr_2−O stretch involving the oxygen atoms of axially ligated THF.

The persistence of RR intensity for the dmp aromatic ring modes throughout the visible−excitation range, compared with those arising from the saturated portion of the ligand, is clear evidence that the π system of the phenyl ring of dmp is vibronically coupled to the visible electronic transition(s), while the increasing dominance of the a, b, and c bands as the laser excitation is tuned toward the blue strongly suggests a metal-

(24) Morris, D. E.; Woodruff, W. H. *J. Phys. Chem.* **1985**, *89*, 5795.

(25) Dollish, F. R.; Fateley, W. G.; Bentley, F. F. *Characteristic Raman Frequencies of Organic Compounds*; John Wiley & Sons: New York, 1974.

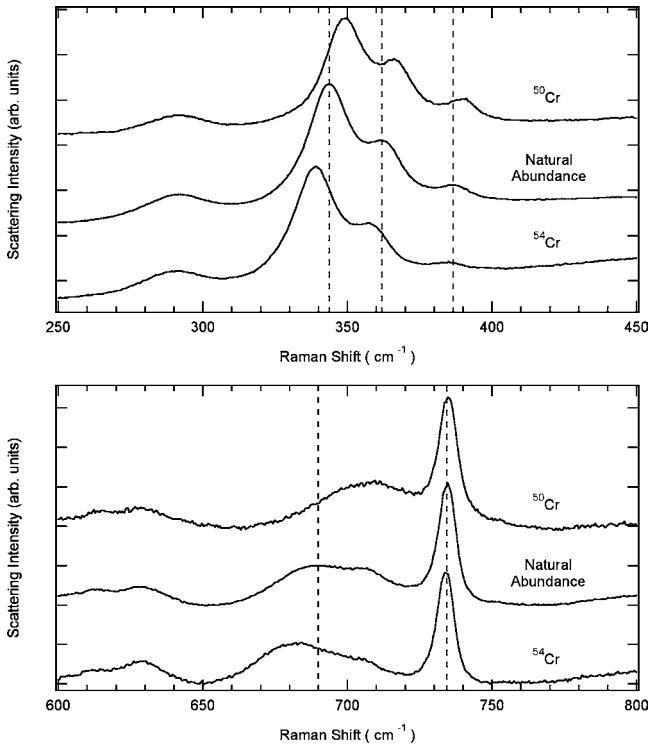

Figure 7. Resonance Raman (488 nm) spectra of $Cr_2(dmp)_4$ isotopomers.

centered transition. One interpretation of this behavior is that there are two types of electronic transitions, e.g., MLCT (or LMCT) and $\delta \rightarrow \delta^*$, giving rise to resonance enhancement of vibrations on different parts of the molecular structure.

This interpretation is not necessarily correct, however. Several of the results cited in the previous section suggest strong $d\pi$(metal)−$p\pi$(ligand) interactions in the Cr complex that are weak or absent for Mo. In the ground state there can be direct $d\pi-p\pi$ bonding between the chromium d-orbitals having δ symmetry with respect to the Cr−Cr axis but π symmetry with respect to the Cr−C(phenyl) bond. The spectra suggest that either poor spatial overlap or mismatch of orbital energies, or both, render $d\pi-p\pi$ bonding unimportant in the Mo complex.

Nevertheless, the Gaussian resolution of the of $Cr_2(dmp)_4$ absorption envelope requires three components. The DFT results suggest that the lowest-energy, weak contributor to the Cr absorbance may be the triplet $\delta \rightarrow \delta^*$ transition. The sparse RR excitation profile data that we report here do not permit us to identify the underlying electronic transitions for either Cr or Mo. Changes of the relative intensity of bands a, b, and c with laser excitation energy probably are selective enhancement effects due to vibronic structure that is unresolved in the room-temperature spectra, but may reflect differing enhancement due to distinct electronic transitions or possibly interference effects.

Chromium Isotope Substitution. The suggestion made above that bands a, b, and c are normal modes containing large contributions from displacement of the Cr−Cr internal coordinate is verified by comparison of the spectra from isotopically substituted $Cr_2(dmp)_4$, including the complex synthesized from natural abundance chromium (∼84% ^{52}Cr), ^{50}Cr, and ^{54}Cr (Figure 7). Isotope shifts are observed in bands a, b, and c, with the ^{54}Cr isotopomer exhibiting frequencies of 338.9, 356.5, and 383.8 cm^{-1} and the corresponding bands in the ^{50}Cr isotopomer at 349.0, 365.9, and 389.4 cm^{-1}. The bottom portion of Figure 7 confirms the overtone assignment to the band at 690 cm^{-1}, as it exhibits an isotope dependence approximately twice that of the fundamental. Similar shifts (not shown) confirm that the bands at 1079 and 1368 cm^{-1} are combinations of bands with the aromatic bending and breathing modes, respectively. Finally, in the bottom panel, a slight (∼1 cm^{-1}) but clear dependence of the aromatic ring deformation mode at 734 cm^{-1} on metal isotope is also seen. We suggest that the isotope data, along with the aforementioned RR enhancement patterns and the perturbations of both the high-frequency and low-frequency regions of the $Cr_2(dmp)_4$ spectrum compared to that of the Mo complex, constitute *prima facie* evidence for highly mixed normal modes in the Cr complex, especially involving totally symmetric combinations of the Cr−Cr, Cr−C, and Cr−O internal coordinates. Once again, one might be tempted to conclude that the Cr−Cr stretching frequency, if unmixed, would be near 365 cm^{-1}, but this is inconsistent with the empirical prediction, the DFT results, and also the *aggregate* Cr isotope shift, as we discuss below.

Considering the metal−metal core as a simple diatomic oscillator, the predicted vibrational shift of a 340 cm^{-1} band upon altering the chromium isotope from 54 to 50 would be ∼13 cm^{-1}. (By way of comparison, Shriver and co-workers reported an isotope shift for $Mo_2(O_2CCH_3)_4$ upon substitution of ^{92}Mo for the naturally abundant isotopic mixture that was essentially identical to that predicted for a diatomic structure.[26]) The observed shift of 10 cm^{-1} for band a, and the 9 cm^{-1} shift of band b, are both consistent with substantial contributions of the metal−metal stretch but combine to exceed that expected for a simple diatomic. In fact, the *aggregate* Cr isotope shift of bands a, b, and c is 25.1 cm^{-1}. If we assume that the contribution of the Cr−Cr internal coordinate to the potential energy distribution of normal modes a, b, and c is the sole source of the isotope shifts, then the "natural frequency" of the Cr−Cr stretch, if it were an unmixed mode as in the Mo complex, can be estimated from the aggregate Cr isotope shift as ca. 650 cm^{-1} (force constant 6.54 mdyn/Å). This is in satisfactory agreement with the frequency predicted from the Cr−Cr bond distance via the empirical equations,[16] 700 cm^{-1} (see also Figure 1), and those predicted by the DFT calculations.

Similar three-mode mixing has been observed for $Mo_2(CCR)_4(PMe_3)_4$[27] and $[NEt_4]_4[Mo_2(CN)_8]$.[28] The free ligand Raman spectrum (Li complex, Figure 4) indicates that ligand bending or torsional modes are found in the same general energy range (∼376 cm^{-1}) as bands a, b, and c. However, mode mixing to yield the present result is much more extensive than can be ascribed simply to the energetic similarity of a free ligand coordinate, as indicated by the foregoing discussion and the metal-isotope dependence of the aromatic deformation mode near 730 cm^{-1}. Such mixing generally occurs in complexes where the M−L bond axes are at angles to the M−M axis that differ substantially from 90°, as in, for example, triply bonded M_2L_6 complexes having the ethane structure.[29] In complexes where the M−M−L angles are approximately 90°, as in the present case, the $Mo_2(O_2CCH_3)_4$ example cited above, and numerous other second- and third-row complexes with quadruple metal−metal bonds,[16] the diatomic approximation suffices to

(26) Hutchinson, B.; Morgan, J.; Cooper, C. B., III; Mathey, Y.; Shriver, D. F. *Inorg. Chem.* **1979**, *18*, 2048.
(27) John, K. D.; Miskowski, V. M.; Vance, M. A.; Dallinger, R. F.; Wang, L.; Geib, S. J.; Hopkins, M. D. *Inorg. Chem.* **1998**, *37*, 6858.
(28) Clark, R. J. H.; Firth, S.; Sella, A.; Miskowski, V. M.; Hopkins, M. D. *J. Chem. Soc., Dalton Trans.* **2000**, 2928.

extract the M−M force constant from vibrational data. We suggest, however, that this approximation breaks down for chromium complexes including $Cr_2(dmp)_4$, $Cr_2(mhp)_4$, and $Cr_2(carboxylate)_4$, despite the fact that the Cr−L bond axes are almost orthogonal to the Cr−Cr axis. In structures like this, mixing of the M−M and M−L internal coordinates via kinematic coupling of the M−M and M−L oscillators will be negligible. What, then, is the mechanism that we propose for generating the highly mixed normal modes with contributions from the M−M, M−L, and M−M−L coordinates that we suggest (and the isotope evidence supports) in $Cr_2(dmp)_4$, and does this mechanism have potential generality? The answers lie in the unusual force matrix that we suggest describes the force field for the M−M, M−L, and M−M−L coordinates of $Cr_2(dmp)_4$ and potentially, by implication, other $Cr(II)_2$ complexes with first-row ligands allowing $d\pi-p\pi$ interactions. We have argued, and presented evidence above, that influences of the δ-bond in $Cr_2(dmp)_4$, including ground-state bonding and $\delta\rightarrow\delta^*$ excitation, strongly affect Cr−L bonding, and even bonding within the phenyl ring of dmp, via $d\pi-p\pi$ interactions. We suggest that related effects are at play in the ground-state vibrational force field of this complex. In the vibrational force field, these electronic interactions have the effect of creating off-diagonal force constants in the force matrix[30] that can strongly mix internal coordinates into normal modes, even if the internal coordinates are geometrically orthogonal. We further suggest that similar effects in other complexes can confound identification of a "true" metal−metal stretching frequency (or force constant) and thus lead to ambiguities concerning the nature of metal−metal bonding.

Cr_2 and Mo_2 Systems with Higher Bond Orders. In contrast to the d^4 $M(II)_2$ complexes discussed previously, the gas-phase M(0) diatomic molecules Cr_2 and Mo_2 have formal M−M bond orders of six. Both of these M_2 molecules have "ultrashort" M−M bonds (i.e., the shortest bond lengths known for their respective rows of the Periodic Table), 1.69 Å for Cr_2[31] and 1.93 Å for Mo_2.[32] The force constant of the Mo−Mo bond in Mo_2, 6.44 mdyn/Å (νM−M = 477 cm^{-1} in the $^1\Sigma_g^+$ state), places this molecule precisely on the empirical correlation for its row of the Periodic Table (Figure 1, rightmost point). By comparison, the Cr−Cr stretching frequency in $^1\Sigma_g^+$ Cr_2 is only 480 cm^{-1},[33] which yields a force constant of 3.53 mdyn/Å, far below the empirical correlation for that row and far less than the DFT prediction for the formal quadruple bond in $Cr_2(dmp)_4$ (Table 1). The reason for this may lie in the distorted Cr−Cr potential that some theoretical studies find for Cr_2.[34] While the bonding potential in the Cr(II) dimers is expected to be entirely different from that of Cr(0) Cr_2(g), it must be acknowledged that similar distorted potentials may be responsible for the "anamolous" Cr−Cr frequencies observed in the $Cr(II)_2$ complexes.

Conclusions

The Raman spectroscopy of $Mo_2(dmp)_4$ is straightforward with respect to the assignment of the metal−metal stretch at 424 cm^{-1}, which exhibits strong intensity enhancement in resonance with the $\delta\rightarrow\delta^*$ transition of the Mo_2 moiety. This frequency is one of the highest reported for a Mo_2 quadruply bonded complex, consistent with $Mo_2(dmp)_4$ possessing one of the shortest Mo_2 bonds. Weakly enhanced modes at lower frequency, assigned to M−L stretches and M−M−L angle bends, are also observed. However, the coupling of these modes to the $\delta\rightarrow\delta^*$ chromophore is weak, and the influence of the δ-bond and the $\delta\rightarrow\delta^*$ transition on the electronic structure of the dmp ligand is negligible, as evidenced by the RR enhancement patterns (or lack thereof).

The situation is entirely different in $Cr_2(dmp)_4$. The RR spectra are much more complex, showing persistent enhancement of ligand modes belonging to the phenyl ring of dmp, splitting of ligand phenyl ring modes indicating uniquely strong metal−ligand interactions, and a highly perturbed, intense, and complicated low-frequency region. Most importantly, the $^{50/54}Cr$ isotope data definitively show that the potential energy of the Cr−Cr internal coordinate is distributed among at least three of these low-frequency normal modes, at 344, 362, and 386 cm^{-1} in the natural abundance isotopomer. We suggest that the main additional internal coordinates that contribute to these modes are the Cr−O and Cr−C stretching coordinates and the Cr−Cr−(O,C) angle bends, although low-energy ligand coordinates might also be involved. The major point that we infer is that the "natural frequency" of the Cr−Cr stretching coordinate, if it behaved as a vibrationally unmixed mode as does the Mo−Mo coordinate in $Mo_2(dmp)_4$ instead of being distributed among several normal modes, is much higher than any of the three normal-mode frequencies mentioned above. If we assume that the chromium isotope shifts in these modes occur only to the extent that the Cr−Cr stretching coordinate contributes to the normal modes, then we can estimate the "natural" Cr−Cr frequency from the aggregate $^{50/54}Cr$ isotope shifts of the three modes. This Cr−Cr frequency turns out to be ca. 650 cm^{-1} (diatomic force constant ca. 6.5 mdyn/Å), which is a perfectly reasonable value for a Cr−Cr quadruple bond with substantial δ-bonding. This frequency also is in good agreement with predictions from our DFT calculations and with empirical estimates from our force constant−bond distance relationships, as shown in Figure 1. Despite this evidence, we must acknowledge the possibility that a distorted Cr−Cr potential similar to that inferred for $Cr(0)_2$ may contribute to the vibrational behavior of the $Cr(II)_2$ complexes. Finally, an important general lesson to be gained from this study is that estimation of metal−metal bond frequencies (and thus the nature of the metal−metal bonds themselves) from vibrational or vibronic data needs to be approached with caution when there are strong interactions between M−M and M−L bonds via orbitals that participate simultaneously in metal−metal and metal−ligand bonding, as we have demonstrated in the present case. It appears that elements in the first transition series, most particularly Cr(II), may be especially likely to present this type of situation.

Acknowledgment. The authors gratefully acknowledge the Los Alamos National Laboratory Directed Research and Development

(29) (a) Chisholm, M. H.; Cotton, F. A.; Frenz, B. A.; Reichert, W. W.; Shive, L. W.; Stults, B. R. *J. Am. Chem. Soc.* **1976**, *98*, 4469. (b) Chisholm, M. H.; Cotton, F. A.; Extine, M.; Stults, B. R. *J. Am. Chem. Soc.* **1976**, *98*, 4477.
(30) Wilson, E. B., Jr.; Decius, J. C.; Cross, P. C. *Molecular Vibrations*; McGraw-Hill: New York, 1955.
(31) Michalopoulos, D. L.; Geusic, M. E.; Hansen, S. G.; Powers, D. E.; Smalley, R. E. *J. Phys. Chem.* **1982**, *86*, 3914.
(32) Huber, K. P.; Hertzberg, G. *Molecular Spectra and Molecular Structure, IV; Constants of Diatomic Molecules*; Van Nostrand: New York, 1979.
(33) Moskovits, M.; Limm, W.; Mejean, T. *J. Phys. Chem.* **1985**, *89*, 3886.
(34) Dachsel, H.; Harrison, R. J.; Dixon, D. A. *J. Phys. Chem. A* **1999**, *103*, 152.

(LDRD) fund for financial support. LANL is operated by Los Alamos National Security, LLC, for the National Nuclear Security Administration of the U.S. Department of Energy under contract DE-AC52-06NA25396. Additional funding was provided by the U.S. Public Health Service under NIH Grant DK36263 to W.H.W. Dr. Basil I. Swanson (LANL) and Prof. Michael D. Hopkins (University of Chicago) are acknowledged for helpful discussions.

Supporting Information Available: Complete ref 21 and electronic absorption spectra of $Mo_2(dmp)_4$ and $Cr_2(dmp)_4$ at 15 K (mineral oil mull) and at room temperature (THF solution). This information is available free of charge via the Internet at http://pubs.acs.org.

JA9055504